Volume 64, Issue 2, 2020
Journal of Scientific Research
Institute of Science,
Banaras Hindu University, Varanasi, India.

Structural Behavior and Photoluminescence Properties of Ytterbium (III) Doped Lithium Aluminates Prepared via Microwave Assisted Solution Combustion Method

M A Wani and R M Belekar*

Department of Physics, Government Vidarbha Institute of Science and Humanities, Amravati, India-444604.
rajubelekar@gmail.com*

Abstract: **A series of novel temperature-sensitive phosphors $LiAlO_2:Yb^{3+}$ (with Yb^{3+} concentration, 0.01, 0.02 and 0.03 mole %) were synthesized by microwave triggered solution combustion synthesis method. The structural identification and phase determination of the prepared sample were carried out by powder X ray diffraction and FT-IR techniques whereas the physical morphology of the sample was investigated by SEM. The XRD peaks along with rietveld refined data confirms the formation of tetragonal single crystal $LiAlO_2$ with space group P4 12 12 having 92 space group number. All the substituted materials adopt the same structure to that of $LiAlO_2$ indicates that ytterbium ion has been well incorporated in to the crystal lattice without disturbing natural crystal structure of the host. The SEM image of the material shows transparent phosphor with irregular shape and surfaces of the foams shows lot of cracks, voids and micropores. The photoluminescence spectra of ytterbium doped $LiAlO_2$ exhibits absorption and emission due to $^2F_{7/2}$ to $^2F_{5/2}$ transitions. The strong interaction of Yb^{3+} ions within the lattice vibration gives rise to strong vibrational sidebands**.

Index Terms: **$LiAlO_2$, phosphors, Luminescence, Rietveld refinement, SCS method.**

I. INTRODUCTION

In the world of clean and ecofriendly energy sources, phosphors play vital role in designing phosphor lamp, light emitting diodes, lasers, optical amplifiers, medical diagnostics and luminescence sensors etc. (D. Šević, 2020) Usually phosphors are primarily based on luminescent properties of activators typically from different lanthanides series, located in wide-band gap spinel or hosts organized during the course of the synthesis. (KA Gedekar, 2018) Normally host materials ought to exhibit proper mechanical, optical and thermal residences in order to prepare excellent phosphor (Belekar R. M. & Dhoble S. J., 2018). Aluminates form supported with alkali, alkaline earth or rare-earth oxides have high melting point and resistance to chemical attack. (KA Gedekar, 2017) Additionally such ceramics materials have a variety of applications as cements, castable ceramics, bioceramics, and electro ceramics (Ning Xie, 2020).

The $LiAlO_2$ spinel is an optically inert medium and possesses chemical and thermal stability, transparency, mechanical strength, chemical inertness, extensive band gap, low density and excessive melting point increases its beauty for luminescent ions. (Monali R. Kadukar, 2017) Lithium-ion batteries have attracted significant attention nowadays due to higher power and small size (Feixiang Wu, 2020). In typical lithium-ion batteries, energy release mechanism is exhibited due to the diffusion of the delocalized ions, or transfer of lithium ions between an anode and a cathode (Taehoon Kim, 2019). The cathode of such batteries is basically made up of lithium or transition metals such as nickel, cobalt and manganese (R. Jung, 2019). Though lithium-ion batteries find its great application in electric vehicles, but due to the limited life span power efficiency and high cost restrains its widespread deployment of electric vehicles (Shanhai Ge, 2020). To increase the life span and power efficiency, we must dope host material with the nickel or cobalt. The ions will transfer the energy to the host material during the process of diffusion. The charge carriers flows their energy in the system which enhances the power rate (Tianmei Chen, 2020).

In the literature, Lithium aluminates ($LiAlO_2$) spinel matrix exists in various phases like hexagonal α-$LiAlO_2$, monoclinic β-

* Corresponding Author

$LiAlO_2$, and tetragonal γ-$LiAlO_2$ generated at different temperature range (Liu, 2018). The thermodynamically stable crystal phase of any material mostly generated at 1000°C. Out of all phases, the spinal matrix γ-$LiAlO_2$ is mechanically, chemically and thermally stable when operated at higher temperature with remarkable irradiation permanency (Heo Su Jeong, 2016). The host matrix can be prepared via many strategies like sol-gel, co-precipitation, mechanical-chemical procedure, hydrothermal, micro emulsion, conventional combustion technique and solid state reaction (Belekar R. M. & Dhoble S. J., 2018). But all of these methods were complicated and they required greater energy, long time for synthesis and excessive high temperatures which bring non-homogeneous and commonly low surface area solids (Raju M Belekar, 2014).

In order to overcome these complex synthesis methods, we have adopted microwave assisted solution combustion method because it has enormous traits along with simplicity, quick synthesis time and much less quantity of external power required, also it produce powders of oxides more homogeneous, greater crystalline and of better purity (Belekar, 2018).

This technique basically includes the usage of aluminum and lithium nitrates as oxidant and fuel like urea, glycerin and citric acid would be preferred. The prepared suspension solution is then dragged into the microwave oven, heat generated all through the combustion response among oxidant and fuel (reducing agent) that promotes the formation of the phosphor (ZS Khan, 2016). A massive amount of plumes of gases are released throughout this process (CO_2, N_2, H_2O, CO) and is liable for the destruction of agglomerates and the formation of microspores within the material. In case of convection heating process the material formed is non-homogeneous due to formation of temperature gradient (H. Aihara, 2019).

To conquer this trouble we choose microwave triggered combustion technique, where homogeneity is maintained within the material and whole quantity of particles is uniformly warmed, due to this the penetration depths of radiation are commonly high. (Xie Xinxin, 2019) This minimizes the formation of thermal gradients during synthesis. Hence in the present investigation $LiAlO_2$ doped with different rare earth metals of various concentrations can be carried by means of microwave-assisted combustion. The use of various combinations of the fuels like starch, urea and glycerin could be used to synthesize phosphor materials. In the present study we have used urea as fuel because it is safe, relatively cheap, and available in pure form. The photoluminescence exhibited by prepared phosphor will be carried out by monitoring excitation and emission spectrum within the wavelength 240 nm to 1100 nm. Various factors responsible for luminescence observed in ytterbium and trapping parameters were discussed with utmost accuracy. Based on multicolor luminescence, the phosphors may have potential applications for color displays and fluorescent lamp.

II. EXPERIMENTAL

The Ytterbium oxide doped lithium aluminate ($LiAlO_2$) materials was prepared by microwave assisted solution combustion synthesis (SCS) method. The inorganic materials like lithium nitrate [$Li(NO_3)$], aluminium nitrate [$Al(NO_3)_3$], urea (NH_2CONH_2) and Yb_2O_3 (99.99%) from Merck (AR Grade) were used for the synthesis. The activators in the oxide form were first converted into nitrate form by dragging Yb_2O_3 into in concentrated HNO_3. The doping concentration of the dopants were maintained at x= 0.01, 0.02, and 0.03 (mole %). The stoichiometric amount of the initial ingredients were taken corresponding to composition of $LiAlO_2$ and collected into beaker containing in 30ml de-ionized water maintaining uniform stirring. In order to achieve uniform doping, previously prepared homogeneous solution of Yb^{3+} ions added to this mixture drop wise. This solution was then kept on hot plate until more than half of water contents gets evaporated and viscous gel was formed. The prepared suspension solution was kept in microwave oven at 550°C for at least 3 minutes. The heat generated all through the combustion response amongst oxidant and fuel (reducing agent) that promotes the formation of the phosphor with evolution of large amount of flames. The reaction gets complete in two minutes and foamy ash product gets formed. This foamy product was crushed throughout in agate mortar to form homogeneous product to carry further characterizations. $LiAlO_2$:Yb^{3+} samples were annealed at different calcinating temperature at 600°C, 800°C and 1000°C for at least 5 hours to form promising material of well desirable crystal phase. The prepared material was identified by XRD, FT-IR and SEM techniques and crystal structure along with phase was determined by powder XRD technique.

III. CHARACTERIZATION TECHNIQUES

Crystallographic characterization of the prepared sample was carried out using X-ray diffraction (Rigaku Miniflex diffractometer) using Cu Kα radiation, accelerating voltage: 40kV, 15mA, recorded from 10˚ to 80˚. Fourier transformed infrared spectroscopy used to investigate prominent IR absorption peaks for $LiAlO_2$:Yb^{3+}. The morphology and particle size of a synthesized material were investigated by a Philips CM200 scanning electron microscope (SEM) JSM-7600F model with operating voltage 0.1-30kV was used. The photoluminescence excitation and emission spectra were recorded using a spectrophotometer (Model Hitachi F-7000) carried with a 150 W xenon lamp serves as a source of excitation.

IV. RESULTS AND DISCUSSION

Powder x-ray diffraction technique is used to investigate phase purity of typical phosphors of $LiAlO_2:Yb^{3+}$ sintered at different calcinations 600°C, 800°C and 1000°C for 5h is shown in **Fig. 1**. It can be seen that all the peaks of the samples are found to be well matched with the standard JCPDS data file number PDF(#75–0905) which is corresponding to γ-$LiAlO_2$ phase, which indicates the formation of single phase. The diffraction peaks also shows crystalline and single phase nature of the γ-$LiAlO_2$ samples. The γ- $LiAlO_2$ unit cell possesses tetragonal crystalline structure having lattices parameters a = b = 5.1663 Å and c = 6.2703 Å. The space group for $LiAlO_2$ is P41212 having 92 space group, with calculated particle density of 2.615gcm^{-3}, and with each cation coordinated with the oxygen ions in tetrahedral structure (Su Jeong Heo, 2018). The ions of aluminum and oxygen can be viewed into tetrahedral coordination. It can be visualized as each oxygen ion forming the vertices of lithium and aluminum of centered tetrahedron. The ions of the aluminum and oxygen get accommodated at the corners of the tetrahedral. The substituted activator of the rare earth elements on the lattice site does not affect the geometry of the crystal structure (O. Mondal, 2015). The figure 2 represents Rietveld refinement of x-ray diffraction corresponding to $LiAlO_2$ investigated using Fullprof suit program. The fundamental input parameters for Rietveld refinement was provided from the earlier reported data by researchers (Peter T. Dickens, 2017). The figure 2 shows good agreement with observed values and predicted values by rietveld which are uniform. Figure 1 describes the formation and disappearance in the X-ray diffraction of phases at different temperatures besides few unidentified weak peaks. The average crystallite diameter for the prepared sample calculated from XRD peaks broadening using Debye Scherer's equation (Dennis Wiedemann, 2016):

$$D = 0.9\,\lambda / \beta\cos\theta \ldots\ldots\ldots (1)$$

Where λ (1.54Å) is the wavelength of the X-ray radiation and θ is known as Bragg's angle, and β represents the full width at half maxima (FWHM). The lattice parameters is estimated and related to both Laue and Bragg's equation. The calculated average grain diameter of the prepared samples found within ranges from 50 nm to 65 nm.

The lattice constant (a) of tetrahedral structure is calculated from the Bragg's law using following equation.

$$a_{exp} = d_{hkl}\sqrt{h^2 + k^2 + l^2} \ldots\ldots\ldots (2)$$

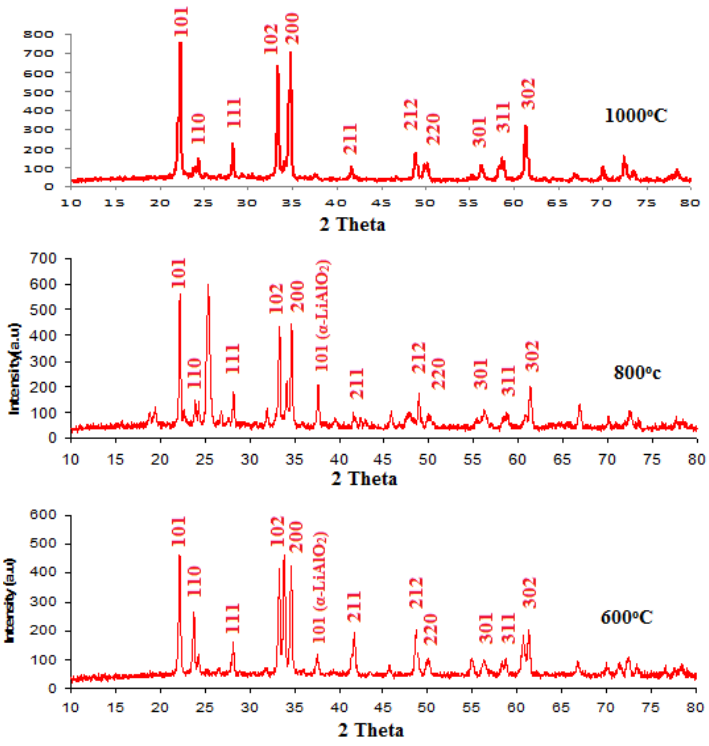

Fig. 1 Shows the XRD diffractogram of $LiAlO_2:Yb^{3+}$ (for Yb^{3+}= 0.01 mole %) sintered at 600˚C, 800˚C and 1000˚C

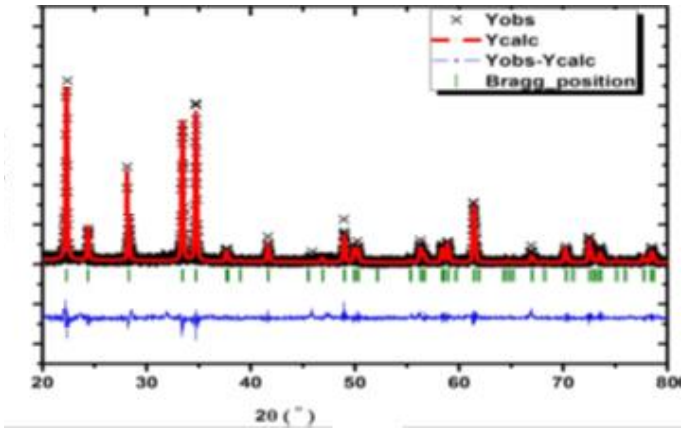

Fig. 2 Rietveld refined XRD pattern of γ-$LiAlO_2$

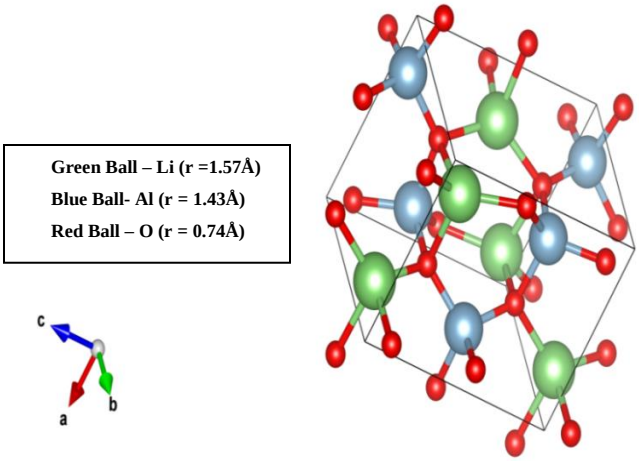

Fig. 3 Primitive cell of LiAlO2

Table 1 Crystallographic parameters for γ -$LiAlO_2$

Crystal Parameters	**Values**
Crystal system	Tetragonal
Crystal space group	$P4_12_12$ (92)
a (Å) = b = (Å) = c = (Å)	5.1663
α (°) = β(°) = γ(°)	90
Volume ($Å^3$)	167.3640

The SEM micrographs of the prepared samples via microwave assisted solution combustion for the doping concentration 0.01 mol. % (ytterbium) are shown in figure 3. The microstructure of the ytterbium doped $LiAlO_2$ ceramic shows transparent in nature makes it suitable luminescence material. As all the samples with different dopant concentrations were prepared by same method, hence surface morphologies with different dopant concentrations are hardly affected (V.D. Mote, 2015). It also indicates that different particle dimensions and shapes were formed. Irregular tetragonal crystals of $LiAlO_2$:Yb^{3+} with grain size 10-20µm was obtained. The SEM micrographs shows irregular shape and size of particles with large number of pores which might due to large amount of gases liberated during combustion reaction between metal nitrates and fuel (Arvind Varma, 2016). It can also be seen from SEM micrograph that few grains possess tetragonal morphology as predicted by X ray diffraction study. In case of solution combustion synthesis, there is flow of mass in irregular fashion during reaction which usually produces highly agglomerated particles involving lot of voids and pores. However there is uniform doping of trace element like rare earth in the host lattice.

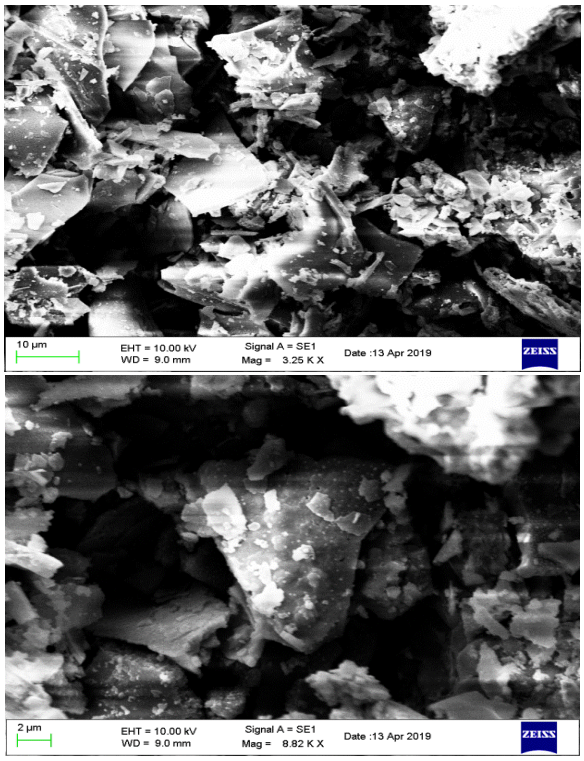

Fig. 4 SEM micro image of $LiAlO_2$ doped with Yb^{3+} (x= 0.01 mole %) sintered at 800℃

Fourier transformed infrared spectroscopy (FTIR) is used to investigate important absorption peaks corresponding to major vibrations in $LiAlO_2$:Yb^{3+} (x= 0.01 mole %) as shown in figure 5 at wavenumber 1100 cm^{-1}, 873 cm^{-1}, and 740 cm^{-1}. The infrared absorption observed at wave number 1100 cm^{-1} represents Al-O vibration stretching mode. The absorption peak at wavelength 873 cm^{-1} exhibits the Li-O mode of vibration. The absorption band observed at wavenumber 1100 cm^{-1} attributed due to Al-O stretching mode vibrations. The strong absorption peaks observed within 700 cm^{-1}-900 cm^{-1} should be assigned to Al-O bending vibrations which assures the presence of Al-O bond in the material. Few absorption peaks beyond 1100 cm^{-1} was also observed which may arise due to varying bond length of Al-O bond. It was worthwhile to note that there were not any peaks observed within 1500 – 2500 cm^{-1} which indicated the complete removal of unreacted nitrates and other organic volatile matter during sintering. The peaks observed at 3300–3500 cm^{-1} is assigned to stretching O-H bond which is attributed due to physically adsorbed water. The FT-IR spectra also shows few bands at wavenumber of 650 cm^{-1} and 810 cm^{-1} which can be assigned to stretching vibration frequencies of AlO_4 tetrahedral whereas few weak absorption bands observed at 520 cm^{-1} and 550 cm^{-1} which are corresponding to AlO_4–LiO_4 lattice vibrations, respectively (Masoud, 2016).

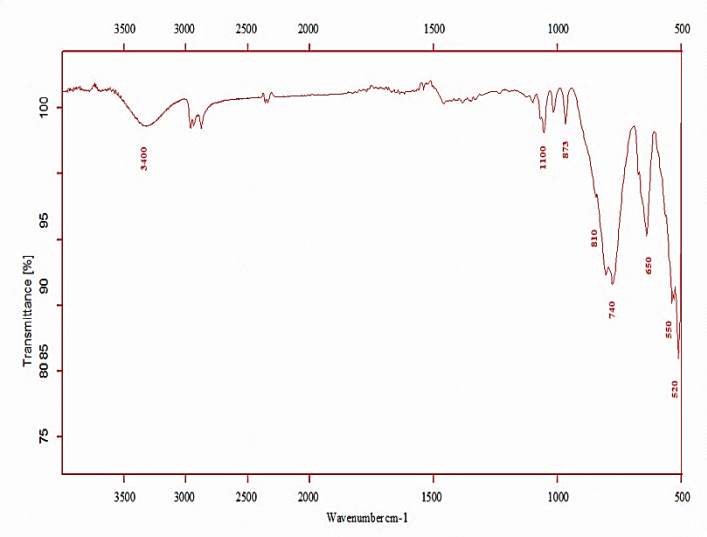

Fig.5 FT-IR spectra of synthesized Ytterbium (III) doped lithium aluminates (0.01 mole %) sintered 800℃

The absorption and emission spectra of $LiAlO_2:Yb^{3+}$ for 0.01 mole % concentration of Yb^{3+} thermally treated at 800˚C are shown in figure 6. The Absorption spectra monitored from 240 nm to 500 nm recorded under UV excitation. The spectrum gives clear look of broad excitation peak observed with maxima centered at 254 nm, which corresponds with band gap of 4.26 eV arise due the defects present in the host lattice. Such wide absorption band is arising due to transition of Yb^{3+} electron present in the band gap area of the host matrix.

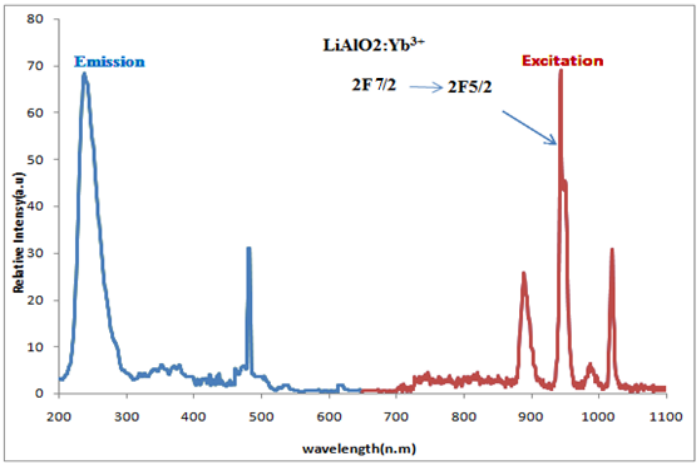

Fig. 6 Luminescence Excitation and Emission spectra of $LiAlO_2:Yb^{3+}$ (for Yb^{3+}= 0.01 mole %)

The emission spectra of $LiAlO_2:Yb^{3+}$ monitored from 650 nm to 1020 nm under UV excitation of 254 nm. The strong electron phonon coupling of Yb^{3+} ion is responsible for the additional peaks which appear in emission spectra band centered at 981 nm. Different absorption and emission lines can be seen due to the different transitions between the two $^2F_{7/2}$ and $^2F_{5/2}$ multiplets (L.Van Pieterson, 2000). This two energy states splits to form seven stark levels, levels 1 to 4 for the ground state $^2F_{5/2}$ and levels 5-7 for the $^2F_{7/2}$ excited state. The peak observed at 1020 nm arises due to the transition from stark level 5 → 1. No significant changes were observed in the photoluminescence spectrum of $LiAlO_2:Yb^{3+}$ for various concentrations of dopants, which might due to the smaller amount of doping variation.

Conclusion

The $LiAlO_2:Yb^{3+}$ phosphors have been successfully synthesized via microwave assisted solution combustion synthesis method. The prepared material was identified and characterized by using powder X-ray diffraction method, SEM, FTIR techniques. The XRD peaks along with rietveld refined data assures the formation of tetragonal single-crystal $LiAlO_2$ with space group P4 12 12 having 92 space group number. All the substituted materials adopt the same structure to that of $LiAlO_2$ indicates that the ytterbium ion has been well incorporated in to the crystal lattice without disturbing natural crystal structure of the host. The SEM micrographs show sponge like agglomerated particles with irregular shape and size (typically 10-20 μm) has sponge like structure with large amount of pores and voids present on the surface of the material which is due to the evolution of enormous amounts of gases during combustion synthesis. In the infrared absorption spectroscopy, absorption bands observed at wave number 1100 cm^{-1} and 873 cm^{-1} represents Al-O and Li-O mode of vibration respectively. In order to study optical properties of the phosphor material, excitation and emission spectra of the phosphor were recorded. The spectrum gives clear look of broad excitation peak observed with maxima centered at 254 nm, which corresponds with band gap of 4.26 eV arise due the defects present in the host lattice. The emission observed at 981 nm and 1020 nm arose due to transitions observed between the two $^2F_{7/2}$ and $^2F_{5/2}$ multiplets.

Conflicts of Interest

The authors of this paper declare no conflict of interest.

References

Arvind Varma, Alexander S. Mukasyan, Alexander S. Rogachev & Khachatur & V. Manukyan. (2016). Solution Combustion Synthesis of Nanoscale Materials. *Chemical Reviews*, 14493-14586.

Belekar, RM. (2018). Structural and Electrical Studies of Nanocrystalline Fe2O3 Prepared by Microwave Assisted Solution Combustion Method with Mixed Fuel Approach. *Journal of Physical Sciences*, 189-199.

Belekar R. M. & Dhoble S. J. (2018). Activated Alumina Granules with nanoscale porosity for water. *Nano-Structures & Nano-Objects*, 16, 322-328.

D. Šević, M. S. Rabasović, J. Križan, S. Savić-Šević, M. D. Rabasović, B. P. Marinkovic & M. G. Nikolic. (2020). Effects of temperature on luminescent properties of

Gd2O3:Er, Yb nanophosphor. *Optical and Quantum Electronics*, 52,5.

Dennis Wiedemann, Suliman Nakhal, Johanna Rahn, Elena Witt, Mazharul M. Islam, Stefan Zander, Paul Heitjans, Harald Schmidt, Thomas Bredow, Martin Wilkening, & Martin Lerch. (2016). Unravelling Ultraslow Lithium-Ion Diffusion in γ-LiAlO2: Experiments with Tracers, Neutrons, and Charge Carriers. *Chemistry of Materials*, 915-924.

Feixiang Wu, Joachim Maier & Yan Yu. (2020). Guidelines and trends for next-generation rechargeable lithium and lithium-ion batteries. *Chemical Society Reviews*, 1569-1614.

H. Aihara, J. Zider, G. Fanton & T. Duerig. (2019). Combustion Synthesis Porous Nitinol for Biomedical Applications. *International Journal of biomaterials*, 4307461.

Heo Su Jeong, Hu Boxun, Manthina Venkata, Hilmi Abdelkader & Yuh Chao-Yi, Surendranath Arun & Singh Prabhakar. (2016). Stability of lithium aluminate in reducing and oxidizing atmospheres at 700 C. *International Journal of Hydrogen Energy*, 10.1016/j.ijhydene.2016.03.145.

KA Gedekar, SP Wankhede, SV Moharil & RM Belekar. (2017). d–f luminescence of Ce3+ and Eu2+ ions in BaAl2O4, SrAl2O4 and CaAl2O4 phosphors. *Journal of Advanced Ceramics*, 341-350.

KA Gedekar, SP Wankhede, SV Moharil & RM Belekar. (2018). Synthesis, crystal structure and luminescence in Ca3Al2O6. *Journal of Materials Science: Materials in Electronics*, 6260-6265.

L.Van Pieterson, M. Heeroma, E. De Heer & A. Meijerink. (2000). Charge transfer luminescence of Yb3+. *Journal of Luminescence*, 177-193.

Liu, Guangtao Liu & Hanyu. (2018). First principles study of LiAlO2: new dense monoclinic phase under high pressure. *Journal of Physics: Condensed Matter*, 115401.

MA Wani, RM Belekar & BA Shingade. (2019). Study of photoluminescence properties of MgAl2O4 doped with europium prepared by microwave assisted solution combustion synthesis. *AIP Conference Proceedings*, 030003.

Masoud & Emad M. (2016). Nano lithium aluminate filler incorporating gel lithium triflate polymer composite: Preparation, characterization and application as an electrolyte in lithium ion batteries,. *Polymer Testing*, 65-73.

Monali R. Kadukar, P. W. Yawalkar, S. P. Lochab, S. J. Dhoble & B. Sudhakar Reddy. (2017). Thermoluminescence and kinetic study of low z LiAlO2:Dy/Eu phosphors. *Ferroelectrics Letters Section*, 1-3, 8-17.

Ning Xie, Chengguo Ming, Yanming Hao & Manting Pei. (2020). Photo-luminescence characteristics of binary P2O5–CaO glass ceramic. *Materials Science and Technology*, 726-730.

O. Mondal, M. Pal, R. Singh, D. Sen, S. Mazumder & M. Pal. (2015). Influence of doping on crystal growth, structure and optical properties of nanocrystalline CaTiO3: a case study using small-angle neutron scattering. *Journal of Applied Crystallography*, 836-843.

Peter T. Dickens, José Marcial, John McCloy, Benjamin S. McDonald & Kelvin G. Lynn,. (2017). Spectroscopic and neutron detection properties of rare earth and titanium doped LiAlO2 single crystals,. *Journal of Luminescence*, 242-248.

R. Jung, F. Linsenmann, R. Thomas, J. Wandt, S. Solchenbach, F. Maglia, C. Stinner, M. Tromp & H. A. Gasteiger. (2019). Nickel, manganese, and cobalt dissolution from Ni-rich NMC and their effects on NMC622-graphite cells. *Journal of The Electrochemical Society*, A378–A389.

Raju M Belekar, PS Sawadh & RK Mahadule. (2014). Synthesis and structural properties of Al2O3-ZrO2 nano composite prepared via solution combustion synthesis. *International Journal of Research in Engineering & Technology*, 145-152.

Shanhai Ge, Yongjun Leng, Teng Liu, Ryan S. Longchamps, Xiao-Guang Yang, Yue Gao, Daiwei Wang, Donghai Wang & Chao-Yan. (2020). A new approach to both high safety and high performance of lithium-ion batteries. *Science Advances*, eaay7633.

Su Jeong Heo, Rohit Batra, Rampi Ramprasad & Prabhakar Singh. (2018). Crystal Morphology and Phase Transformation of LiAlO2: Combined Experimental and First-Principles Studies. *The Journal of Physical Chemistry C*, 28797-28804.

Taehoon Kim, Wentao Song, Dae-Yong Son,Luis K. Ono & Yabing Qi. (2019). Lithium-ion batteries: outlook on present, future, and hybridized technologies. *Journal of Materials Chemistry A*, 2942-2964.

Tianmei Chen, Yi Jin, Hanyu Lv, Antao Yang, Meiyi Liu, Bing Chen, Ying Xie & Qiang Chen. (2020). Applications of Lithium-Ion Batteries in Grid-Scale Energy Storage Systems. *Transactions of Tianjin University*.

V.D. Mote, J.S. Dargad, Y. Purushotham & B.N. Dole. (2015). Effect of doping on structural, physical, morphological and optical properties of Zn1−xMnxO nano-particles. *Ceramics International*, 15153-15161.

Xie Xinxin, Zhou Yanping & Huang Kama. (2019). Advances in Microwave-Assisted Production of Reduced Graphene Oxide. *Frontiers in Chemistry*, 355.

ZS Khan, NB Ingale & SK Omanwar. (2016). Synthesis and luminescence studies of NaSr4(BO3)3: Dy3+ phosphors. *Optik-International Journal for Light and Electron Optics*, 6062-6065.

***